Synthesis, Structures, and Catalytic Properties of Two Silver(I) Coordination Polymers Constructed from 1,4-Bis(benzimidazolyl)butane

Cui-Hong He, Jin-Ming Hao, Shu-Lin Xiao, and Guang Hua Cui

College of Chemical Engineering, Hebei United University, Tangshan, 063009, P. R. China

Reprint requests to Prof. G.-h. Cui. E-mail: tscghua@126.com

Z. Naturforsch. **2013**, *68b*, 1207 – 1213 / DOI: 10.5560/ZNB.2013-3115
Received April 10, 2013

Using a hydrothermal synthesis method, two silver(I) complexes, $[Ag(bbbm)(1,3\text{-HBDC})]_n$ (**1**) and $[Ag(bbbm)(1,2\text{-HBDC})]_n$ (**2**) (bbbm = 1,1′-(1,4-butanediyl)bis-1*H*-benzimidazole, 1,3-H_2BDC = 1,3-benzenedicarboxylic acid, 1,2-H_2BDC = 1,2-benzenedicarboxylic acid), have been synthesized and characterized by elemental analysis, IR spectra, thermogravimetric (TG) analysis and single-crystal X-ray diffraction. The silver centers display different environments with a distorted T-shaped geometry in **1**, and a linear geometry in **2**. Both chain structures of **1** and **2** are bridged by bbbm in a bis-monodentate coordination mode. **1** is further linked to generate a 3D supramolecular architecture *via* π-π stacking interactions and intermolecular O–H···O hydrogen bonding. In **2**, the ribbon-like chains are additionally assembled by two π-π stacking modes to form a layer motif. The photoluminescence of **1** and **2** was investigated in the solid state. **1** and **2** possess a remarkable activity for degradation of methyl orange by persulfate in a Fenton-like process.

Key words: Azo Dye, Bis(benzimidazolyl)butane, Catalysis, Crystal Structure, Photoluminescence, Phthalic Acid, Silver

Introduction

Research on the design and synthesis of metal-organic frameworks (MOFs) in recent years has become an active area of crystal engineering and supramolecular chemistry, not only for their potential applications in luminescent devices, chemical separation, catalysis, and gas storage, but also for their intriguing variety of architectures and topologies [1 – 3]. Most MOFs are constructed by the assembly of metal ions with an appropriate organic ligand, especially a bridging ligand containing nitrogen, oxygen, or sulfur atoms [4]. The bridging ligands are one of the most important factors that influence the structure of MOFs and their supramolecular architectures. Among them, the flexible α,ω-bis(benzimidazolyl)alkane ligands which contain both the imidazole ring and a larger conjugated π system are excellent components for the construction of extended architectures, as the two benzimidazole rings can freely twist around the flexible -$(CH_2)_n$- spacer to meet the requirements of the coordination geometries of the metal atoms in the assembly process [5 – 10]. Their abilities to act as hydrogen donors as well as in π-π stacking interactions render them good candidates for the construction of supramolecular networks. In order to make good progress in understanding how the nature of metal ions and carboxylate anions affect the architectures, we selected 1,4-bis(benzimidalzolyl)butanes as a nitrogen-donor linker, and two benzenedicarboxylic acid isomers (1,3-, and 1,2-H_2BDC) were used as auxiliary ligands to investigate the influence of different positions of carboxylate anions on the formation of silver(I) complexes. After the mixture had reacted with Ag(I) ions in a hydrothermal process, we obtained and further characterized two infinite chain Ag(I) coordination polymers, namely, $[Ag(bbbm)(1,3\text{-HBDC})]_n$ (**1**) and $[Ag(bbbm)(1,2\text{-HBDC})]_n$ (**2**).

Experimental Section

Materials and characterization methods

All the reagents and solvents for the syntheses were commercially available and used directly without further purification. The ligand bbbm was synthesized according to a literature method [11]. Elemental analyses of C, H, N were

carried out with a Perkin-Elmer 240C elemental analyzer. The IR spectra were obtained on a Bruker Tensor 27 FT-IR spectrometer using KBr pellets in the 4000 – 400 cm^{-1} range. Thermal analyses were performed on a Netzsch TG 209 thermal analyzer from room temperature to 800 °C under nitrogen atmosphere with a heating rate of 10 °C min^{-1}. Luminescence spectra for the solid samples were determined with a Cary Eclipse fluorescence spectrophotometer.

*Synthesis of [Ag(bbbm)(1,3-HBDC)]$_n$ (**1**)*

A mixture of AgOAc (35 mg, 0.2 mmol), 1,3-H_2BDC (33 mg, 0.2 mmol), bbbm (58 mg, 0.2 mmol), and H_2O (18 mL) was sealed in a 25 mL Teflon-lined autoclave and heated to 140 °C for 3 d under autogenous pressure. After the mixture was cooled to room temperature at a rate of 5 °C h^{-1}, colorless block-shaped crystals of **1** were obtained with 47 % yield based on Ag. – Anal. for $C_{26}H_{23}AgN_4O_4$ (563.35): calcd. C 55.43, H 4.12, N 9.95; found C 55.33, H 4.01, N 9.73 %. – FTIR (KBr pellet, cm^{-1}): ν = 3087 w, 2929 w, 1700 s, 1612 m, 1502 s, 1459 m, 1380 m, 1284 w, 1249 m, 1192 m, 1017 m, 747 s, 673 w.

*Synthesis of [Ag(bbbm)(1,2-HBDC)]$_n$ (**2**)*

The synthesis of block-shaped colorless crystals of **2** followed the same procedure as for **1** except that 1,3-H_2BDC was replaced with 1,2-H_2BDC. Yield: 40 % (based on Ag). – Anal. for $C_{26}H_{23}AgN_4O_4$ (563.35): calcd. C 55.43, H 4.12, N 9.95; found C 55.25, H 4.05, N 10.21 %. – FTIR (KBr pellet, cm^{-1}): ν = 3120 w, 2934 w, 1701 s, 1590 s, 1506 s, 1348 s, 1306 w, 1203 m, 1164 m, 1022 m, 782 m, 740 s, 613 m.

X-Ray crystallography

The powder X-ray diffraction pattern was recorded on a Rigaku D/Max-2500 diffractometer at 40 kV, 100 mA for a Cu target tube and a graphite monochromator.

Intensity data for the two complexes were collected at 293 K on a Bruker Smart 1000 CCD diffractometer with graphite-monochromatized MoK_α radiation (λ = 0.71073 Å). Data reduction and absorption corrections were carried out with the programs SAINT and SADABS [12]. The structures were solved by Direct Methods and refined by full-matrix least-squares based on F^2 using the SHELXTL program package [13]. All non-hydrogen atoms were refined with anisotropic displacement parameters. Hydroxyl H atoms of anions were located on a difference Fourier map, while other hydrogen atoms were included in calculated positions and refined with isotropic displacement parameters riding on the corresponding parent atoms. However, the crystal of **1** was not of good quality which led to a data set with many "unobserved" reflections (about 50 %), a large R_{int} and a poor ratio of parameters to reflections. Crystallographic data for **1** and **2** are listed in Table 1. Selected bond lengths and angles for **1** and **2** are listed in Table 2.

Table 1. Crystallographic data and data collection and structure refinement parameters for **1** and **2**.

Complex	**1**	**2**
Empirical formula	$C_{26}H_{23}AgN_4O_4$	$C_{26}H_{23}AgN_4O_4$
M_r	563.35	563.35
Crystal system	orthorhombic	monoclinic
Space group	*Pnma*	$P2_1/c$
a, Å	13.612(4)	7.8090(10)
b, Å	18.014(5)	12.9022(17)
c, Å	9.503(3)	23.760(3)
β, deg	90	104.932(4)
V, Å^3	2330.2(12)	2313.1(5)
Z	4	4
$D_{calcd.}$, g cm^{-3}	1.61	1.62
μ, mm^{-1}	0.9	0.9
F(000), e	1144	1144
Reflections collected / unique	11 303 / 2123	13 864 / 5284
R_{int}	0.1604	0.0564
GOF	1.032	0.956
R_1, wR_2 [$I > 2\,\sigma(I)$]	0.0699 / 0.2385	0.0458 / 0.1096
$\Delta\rho_{max/min}$, e Å^{-3}	0.60 / −0.81	0.42 / −0.53

Table 2. Selected bond lengths (Å) and angles (deg) for **1** and **2**[a].

Complex **1**			
Ag1–N1	2.150(8)	Ag1–N1A	2.150(8)
Ag1–O2	2.480(10)	N1–Ag1–N1A	152.1(5)
N1–Ag1–O2	103.9(3)	N1A–Ag1–O2	103.9(3)
Complex **2**			
Ag1–N1	2.104(3)	Ag1–N3E	2.110(3)
N1–Ag1–N3E	168.08(13)		

[a] Symmetry codes: A: x, $1/2-y$, z; E: $x+1$, $3/2-y$, $z+1/2$.

CCDC 917950 and 917951 contain the supplementary crystallographic data for this paper. These data can be obtained free of charge from The Cambridge Crystallographic Data Centre *via* www.ccdc.cam.ac.uk/data_request/cif.

Catalysis experiments

The catalytic activities were tested with 150 mL aqueous methyl orange solution (10 mg L^{-1}) containing 5 mg of sodium persulfate and 50 mg of **1** or **2** as catalysts [14]. The degradation experiments were performed at 45 °C, and the pH was adjusted to 3 with sulfuric acid (1 mol L^{-1}). Samples of the suspension were withdrawn and analyzed periodically by a Shanghai Jingke 722N UV/Vis spectrophotometer at 506 nm after filtration with 0.45 μm micropore filters. Control experiments without any catalyst were conducted under the same conditions. The degradation efficiency of methyl

orange was calculated based on the following formula:

$$\text{Degradation efficiency} = \frac{(C_0 - C_t)}{C_0} \times 100\,\% \qquad (1)$$

where C_t (mg L^{-1}) is the concentration of methyl orange at reaction time (min), C_0 (mg L^{-1}) is the initial concentration of methyl orange.

Results and Discussion

Description of the crystal structures

*[Ag(bbbm)(1,3-HBDC)]$_n$ (**1**)*

Single-crystal X-ray diffraction analysis reveals that **1** crystallizes in the orthorhombic space group *Pnma* with $Z = 4$. The asymmetric unit of **1** contains one crystallographically independent Ag(I) cation, one half neutral bbbm ligand and one 1,3-HBDC anion. The Ag atom lies on a mirror plane as does the anion, and the entire ligand bbbm is located on a center of inversion. Fig. 1a depicts the coordination environment of the Ag(I) center, showing that it is coordinated by two nitrogen atoms from two distinct bbbm ligands [Ag1–N1 = Ag1–N1A = 2.150(8) Å, N1–Ag1–N1A = 152.1(5)°] and one oxygen atom from a 1,3-HBDC anion [Ag1–O2 = 2.480(10) Å], resulting in a distorted T-shaped geometry [N1–Ag1–O2 = N1A–Ag1–O2 = 103.9(3)°] (symmetry code A: x, $1/2 - y$, z). The bond lengths and angles in **1** are within the normal range observed in other silver bis(benzimidazole) complexes [15–20]. The bbbm ligands act in a typical bis-monodentate mode to connect adjacent Ag(I) atoms generating an infinite chain structure with the Ag···Ag distance being 12.08 Å and the Ag···Ag···Ag angle being 96.347(2)°. These chains are further assembled into the 2D supramolecular structure by π-π stacking interactions between benzene and imidazole rings of different bbbm ligands with the interplanar separation being 3.426 Å and centroid-centroid and slippage distances of 3.717 and 1.442 Å, respectively (Fig. 1b). In addition, the 2D supramolecular structure is extended into a 3D framework *via* strong O–H···O intermolecular hydrogen bonds between the H atom (H1A) of a protonated carboxylic group and an oxygen atom (O3B, symmetry code B: $x - 1/2$, y, $-z + 1/2$) of uncoordinated carboxylate group from a 1,3-HBDC ligand (O1···O3B = 2.495 Å, O1–H1A···O3B = 166.7°).

*[Ag(bbbm)(1,2-HBDC)]$_n$ (**2**)*

Compound **2** crystallizes monoclinically in the space group $P2_1/c$ with $Z = 4$. The asymmetric unit consists of one Ag(I) ion, one bbbm ligand and one uncoordinated 1,2-HBDC anion (Fig. 2a). Each Ag(I) ion is coordinated in a linear geometry with two nitrogen atoms from two bbbm ligands [Ag1–N1 = 2.104(3) Å, Ag1–N3E = 2.110(3) Å] (symmetry code

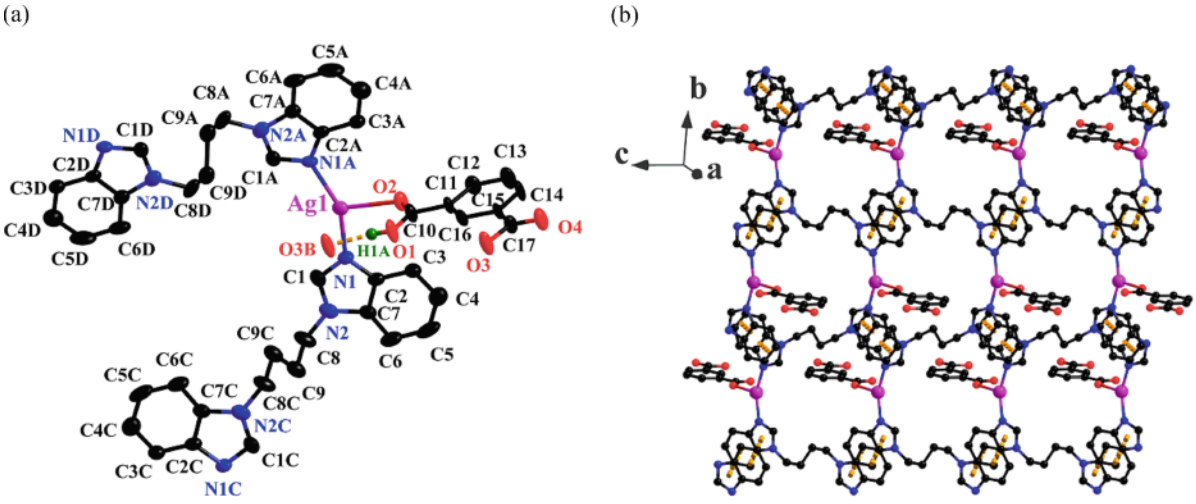

Fig. 1. (a) The coordination environment of the Ag(I) center in **1** with 30 % displacement ellipsoids (symmetry code: A: x, $1/2 - y$, z; B: $1/2 + x$, $1/2 - y$, $1/2 - z$; C: $-x$, $-y$, $1 - z$; D: $-x$, $1/2 + y$, $1 - z$); (b) the 2D supramolecular network of **1** extended by π-π stacking interactions.

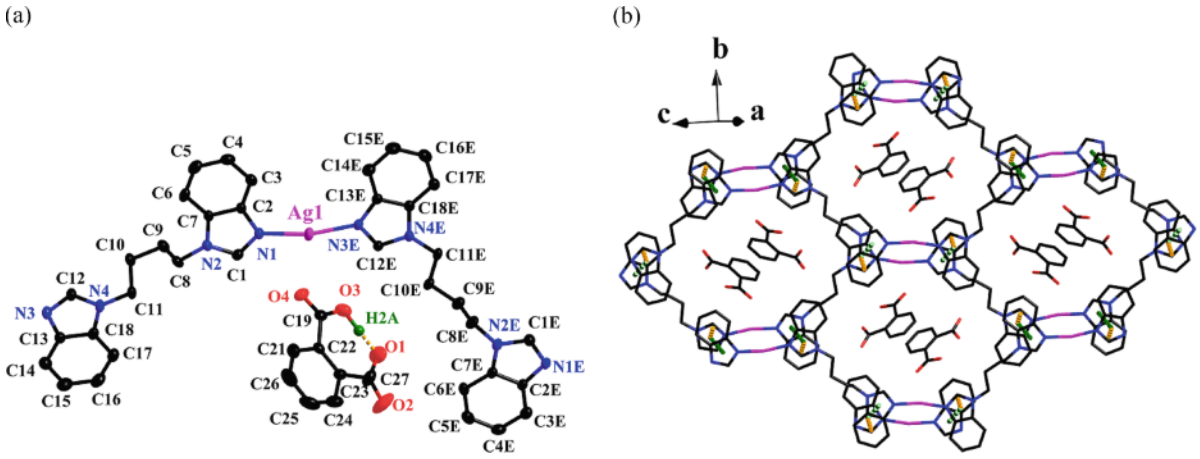

Fig. 2. (a) The coordination environment of the Ag(I) center in **2** with 30% displacement ellipsoids (symmetry code: E: $x+1$, $3/2-y$, $z+1/2$); (b) the 2D supramolecular structure of **2** formed by two modes of π-π stacking interactions. The uncoordinated 1,2-HBDC ligands are filled in the voids.

E: $x+1$, $3/2-y$, $1/2+z$) with the angle N1–Ag–N1E being 168.08(13)°, forming a ribbon-like chain. It is noteworthy that the protonated carboxylic groups of the 1,2-HBDC unit in **2** form a strong intra-anionic O–H···O hydrogen bond (O3···O1 = 2.353 Å, O3–H2A···O1 = 177°) which reduces the coordinative bonding capabilities as compared to 1,3-HBDC in **1**. Adjacent ribbon-like chains are further extended into a 2D supramolecular network through two modes of π-π interaction (Fig. 2b). One is between imidazole rings with an interplanar separation of 3.439 Å (centroid-centroid and slippage distances of 3.655 and 1.238 Å), and another is between imidazole and benzene rings with an interplanar separation of 3.429 Å (centroid-centroid and slippage distances of 3.579 and 1.025 Å).

Powder X-ray diffraction, infrared spectra and thermal analysis

The experimental and computer-simulated powder X-ray diffraction patterns of **1** and **2** show very good agreement (Fig. 3a, b).

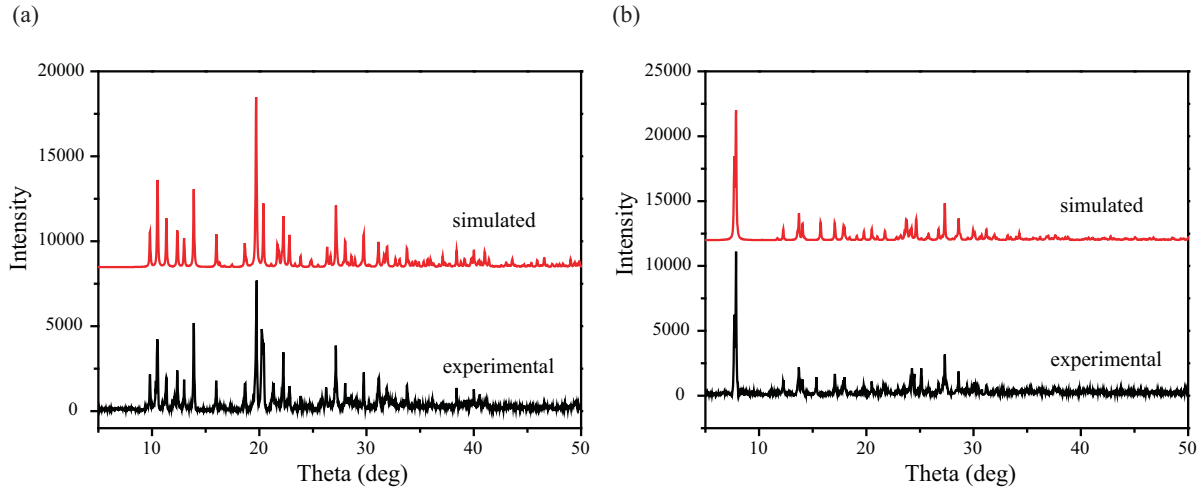

Fig. 3. Powder X-ray diffraction patterns of (a) **1** and (b) **2**.

The main characteristics of the IR spectra of **1** and **2** concern the bbbm ligand and the carboxylate groups of the 1,3-HBDC or 1,2-HBDC ligands. The bands at 1700 and 1701 cm^{-1} belong to -COOH vibrations of 1,3-HBDC and 1,2-HBDC, respectively. Complex **1** also shows characteristic bands of the carboxyl group at 1612 cm^{-1} for antisymmetric and at 1380 cm^{-1} for symmetric stretching. The separation ($\Delta\nu$) between ν_{asym} (COO^-) and ν_{sym} (COO^-) indicates the existence of a monodentate (232 cm^{-1}) coordination mode of the carboxyl group [21]. The characteristic bands at 1502, 1192 and 1017 cm^{-1} for **1** and 1506, 1203 and 1022 cm^{-1} for **2** are assigned to benzimidazolyl ring vibrations.

Thermogravimetric analysis was performed to measure the thermal stabilities of **1** and **2**. The complexes are thermally stable up to 270 °C for **1** and 225 °C for **2**, respectively.

Photoluminescence properties

Luminescent compounds constructed of d^{10} metal centers and organic ligands are of great interest because of their potential applications in chemical sensors and photochemistry [22, 23]. The photoluminescence of **1**, **2** and of the free bbbm ligand was measured in the solid state at room temperature. Their emission spectra are shown in Fig. 4.

The free bbbm ligand displays luminescence with an emission maximum at 368 nm upon excitation at 350 nm, which can be assigned to $\pi \rightarrow \pi^*$ transitions [24, 25]. Peaks at about 371 and 436 nm are found in the emission spectra of **1** and **2** when they are excited at 336 and 338 nm, respectively. The benzenedicarboxylate isomers (1,3- and 1,2-HBDC) show very weak $n \rightarrow \pi^*$ transitions and contribute little to the photoluminescence of the title complexes at room temperature [26]. The emission of **1** is similar to that of the free bbbm ligand, which is probably due to the intraligand $\pi \rightarrow \pi^*$ charge transitions [27, 28]. For **2**, there is an obvious red-shift (68 nm) relative to 1,2-HBDC and bbmb ligands, which may be attributed to ligand-to-metal charge-transfer (LMCT) or intraligand $\pi \rightarrow \pi^*$ charge transitions [29]. Furthermore, the fluorescence intensity of complexes **1** and **2** is much stronger than that of the bbbm ligand. A possible explanation may be the big conformational rigidity of the solid-state complexes in a multidimensional supramolecular network constructed by the cooperative association of coordination as well as hydrogen bonding and π-π stacking interactions in the crystal.

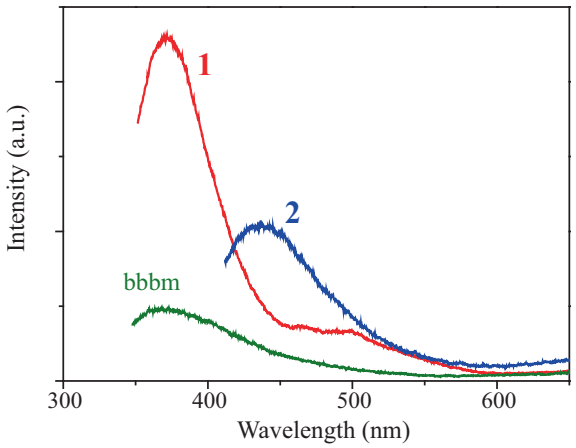

Fig. 4. The emission spectra of complexes **1** and **2** and of the free ligand bbbm.

Catalytic properties

Azo dyes represent more than 50 % of all dyes in common use because of their chemical stability and versatility [30]. However, most of them are non-biodegradable, toxic and potentially carcinogenic. Advanced oxidation technologies utilize persulfate which generates sulfate radicals that are very effective in degrading organic pollutants, but the uncatalyzed reaction rates are generally slow at ambient temperature, and activation of persulfate is necessary to accelerate the process [31, 32]. It has been reported that the

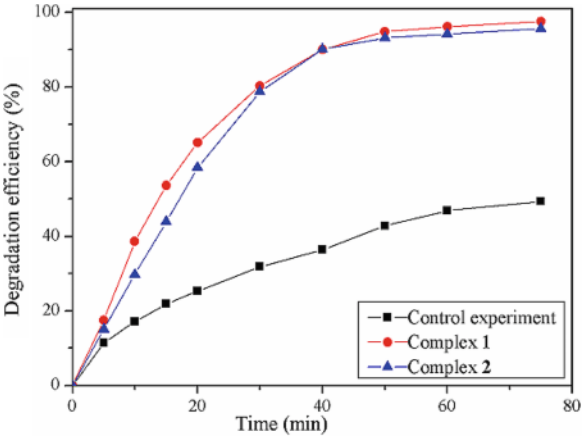

Fig. 5. The experimental results of the degradation of methyl orange.

persulfate anion can thermally or chemically be activated by transition metal ions. So, we employed the two silver(I) coordination polymers as heterogeneous catalysts to activate persulfate anions for chemical oxidation of the azo dye methyl orange in a simulated wastewater (Fig. 5). It is obvious that both complexes have high activity in catalyzing the degradation of methyl orange. The catalytic activities of both **1** and **2** are stable and could be maintained for 40 min with a degradation efficiency of 90 %. Thereafter the reaction is slow and ceases. Within 75 min the efficiencies are about 98 % for **1** and 96 % for **2**. In a control experiment the degradation efficiency is reduced to 49 % in 75 min. **1** and **2** display a remarkable catalytic activity for degradation of methyl orange in the Fenton-like process.

It is possible to describe the mechanism according to Eqs. 2–4 [32].

$$S_2O_8^{2-} + Ag^+ \rightarrow Ag^{2+} + SO_4^{2-} + SO_4^{\bullet -} \quad (2)$$

$$Ag^{2+} + S_2O_8^{2-} \rightarrow Ag^+ + 2\,SO_4^{\bullet -} \quad (3)$$

$$\text{Dye} + SO_4^{\bullet -} \rightarrow \text{oxidation products} \quad (4)$$

Conclusion

In summary, two new silver(I) coordination polymers constructed from the flexible bbbm ligand and two benzenedicarboxylic acids with different positions of the carboxylic groups have been synthesized under hydrothermal conditions. As expected, the results indicate that the position of the carboxylate groups of the aromatic polycarboxylates and supramolecular interactions play an important role in the construction of the title complexes. The photoluminescence studies have shown that the complexes may be candidates for photoactive materials. The two compounds exhibit high catalytic activity in a Fenton-like process for the degradation of methyl orange activated by persulfate.

[1] K. K. Tanabe, S. M. Cohen, *Chem. Soc. Rev.* **2011**, *40*, 498.
[2] S. Pramanik, C. Zheng, X. Zhang, T. J. Emge, J. Li, *J. Am. Chem. Soc.* **2011**, *133*, 4153.
[3] R. Custelcean, *Chem. Soc. Rev.* **2010**, *39*, 3675.
[4] R. Wang, L. Han, F. Jiang, Y. Zhou, D. Yuan, M. Hong, *Cryst. Growth Des.* **2005**, *5*, 129.
[5] G. H. Cui, J. R. Li, J. L. Tian, X. H. Bu, S. R. Batten, *Cryst. Growth Des.* **2005**, *5*, 1775.
[6] H. Jiang, Y. Y. Liu, J. F. Ma, W. L. Zhang, J. Yang, *Polyhedron* **2008**, *27*, 2595.
[7] J. C. Geng, C. H. Jiao, J. M. Hao, G. H. Cui, *Z. Naturforsch.* **2012**, *67b*, 791.
[8] L. Qin, S. L. Xiao, X. H. Zheng, G. H. Cui, *Inorg. Chem. Comm.* **2013**, *34*, 71.
[9] J. F. Ma, J. F. Liu, Y. Xing, H. Q. Jia, Y. H. Lin, *J. Chem. Soc., Dalton Trans.* **2000**, *14*, 2403.
[10] J. Yang, J. F. Ma, Y. Y. Liu, S. L. Li, G. L. Zheng, *Eur. J. Inorg. Chem.* **2005**, *11*, 2174.
[11] J. C. Geng, L. Qin, C. H. He, G. H. Cui, *Transition Met. Chem.* **2012**, *37*, 579.
[12] G. M. Sheldrick, SADABS (version 2.03), Program for Empirical Absorption Correction of Area Detector Data, University of Göttingen, Göttingen (Germany) **2004**.
[13] G. M. Sheldrick, *Acta Crystallogr.* **2008**, *A64*, 112.
[14] L. G. Devi, S. G. Kumar, K. M. Reddy, C. Munikrishnappa, *J. Hazard. Mater.* **2009**, *164*, 459.
[15] C. C. Wang, P. Wang, G. S. Guo, *Transition Met. Chem.* **2010**, *35*, 721.
[16] Y. Y. Liu, Y. Y. Jiang, J. Yang, Y. Y. Liu, J. F. Ma, *CrystEngComm* **2011**, *13*, 6118.
[17] S. L. Xiao, G. H. Cui, V. A. Blatov, J. C. Geng, G. Y. Li, *Bull. Korean Chem. Soc.* **2013**, *34*, 1891.
[18] J. W. Wang, G. H. Cui, L. Qin, S. L. Xiao, *Z. Naturforsch.* **2013**, *68b*, 250.
[19] X. L. Lü, H. Wu, J. F. Ma, J. Yang, *Polyhedron* **2011**, *30*, 1579.
[20] H. L. Hsiao, C. J. Wu, W. Hsu, C. W. Yeh, M. Y. Xie, W. J. Huang, J. D. Chen, *CrystEngComm* **2012**, *14*, 8143.
[21] K. Y. N. Chi, F. Y. Cui, Y. Q. Xu, C. W, Hu, *Eur. J. Inorg. Chem.* **2007**, *27*, 4375.
[22] Q. Wu, M. Esteghamatian, N. X. Hu, Z. D. Popovic, G. Enright, Y. Tao, M. D'Iorio, S. Wang, *Chem. Mater.* **2000**, *12*, 79.
[23] C. L. Chen, B. S. Kang, C. Y. Su, *Aust. J. Chem.* **2006**, *59*, 3.
[24] V. W. Yam, K. K. Lo, *Chem. Soc. Rev.* **1999**, *28*, 323.
[25] J. C. Geng, L. Qin, X. Du, S. L. Xiao, G. H. Cui, *Z. Anorg. Allg. Chem.* **2012**, *638*, 1233.
[26] S. S. Chen, Y. Zhao, J. Fan, T. A. Okamura, Z. S. Bai, Z. H. Chen, W. Y. Sun, *CrystEngComm* **2012**, *14*, 3564.
[27] X. Shi, G. S. Zhu, X. H. Wang, G. H. Li, Q. R. Fang, G. Wu, G. Tian, M. Xue, X. J. Zhao, R. W. Wang, S. L. Qiu, *Cryst. Growth Des.* **2005**, *5*, 207.

[28] X. Shi, G. S. Zhu, X. H. Wang, G. H. Li, Q. R. Fang, X. J. Zhao, G. Wu, G. Tian, M. Xue, R. W. Wang, S. L. Qiu, *Cryst. Growth Des.* **2005**, *5*, 341.
[29] B. Valeur, *Molecular Fluorescence: Principles and Applications*, Wiley-VCH: Weinheim **2002**.
[30] M. Neamtu, I. Siminiceanu, A. Yediler, A. Kettrup, *Dyes Pigments* **2002**, *53*, 93.
[31] J. M. Liu, X. Lin, C. J. Wei, L. D. Li, *Microchim. Acta* **2004**, *148*, 267.
[32] A. M. Ocampo, Dissertation, Washington State University, Pullman WA **2009**.